GEOPHYSICS, VOL. 75, NO. 5 (SEPTEMBER-OCTOBER 2010); P. 75A15–75A29, 9 FIGS., 1 TABLE.
10.1190/1.3481775

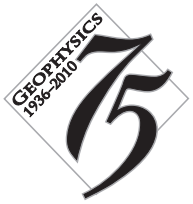

Seismic anisotropy in exploration and reservoir characterization: An overview

Ilya Tsvankin[1], James Gaiser[2], Vladimir Grechka[3], Mirko van der Baan[4], and Leon Thomsen[5]

ABSTRACT

Recent advances in parameter estimation and seismic processing have allowed incorporation of anisotropic models into a wide range of seismic methods. In particular, vertical and tilted transverse isotropy are currently treated as an integral part of velocity fields employed in prestack depth migration algorithms, especially those based on the wave equation. We briefly review the state of the art in modeling, processing, and inversion of seismic data for anisotropic media. Topics include optimal parameterization, body-wave modeling methods, P-wave velocity analysis and imaging, processing in the τ-p domain, anisotropy estimation from vertical-seismic-profiling (VSP) surveys, moveout inversion of wide-azimuth data, amplitude-variation-with-offset (AVO) analysis, processing and applications of shear and mode-converted waves, and fracture characterization. When outlining future trends in anisotropy studies, we emphasize that continued progress in data-acquisition technology is likely to spur transition from transverse isotropy to lower anisotropic symmetries (e.g., orthorhombic). Further development of inversion and processing methods for such realistic anisotropic models should facilitate effective application of anisotropy parameters in lithology discrimination, fracture detection, and time-lapse seismology.

INTRODUCTION

The area of applied seismic anisotropy is undergoing rapid transformation and expansion. Whereas the theoretical foundation for describing anisotropic wave propagation had been developed a long time ago, the multiparameter nature of anisotropic models had precluded their widespread application in seismic exploration and reservoir monitoring. The role of anisotropy has dramatically increased over the past two decades due to advances in parameter estimation, the transition from poststack imaging to prestack depth migration, the wider offset and azimuthal coverage of 3D surveys, and acquisition of high-quality multicomponent data. Currently, many seismic processing and inversion methods operate with anisotropic models, and there is little doubt that in the near future anisotropy will be treated as an inherent part of velocity fields.

A detailed historical analysis of developments in seismic anisotropy can be found in Helbig and Thomsen (2005), so here we mention just several milestones. The work of Crampin (1981, 1985), Lynn and Thomsen (1986), Willis et al. (1986), Martin and Davis (1987), and others convincingly demonstrated that anisotropy has a first-order influence on shear and mode-converted PS-waves, which split into the fast and slow modes with orthogonal polarizations. Shear-wave processing based on Alford (1986) rotation and its modifications has helped document ubiquitous azimuthal anisotropy in the upper crust typically caused by near-vertical systems of aligned fractures and microcracks. Acquisition and processing of high-quality multicomponent offshore surveys starting in the mid-1990s clearly showed that PP- and PS-wave sections could not be tied in depth without making the velocity model anisotropic.

In contrast, anisotropy-induced distortions in P-wave imaging (the focus of the majority of exploration surveys) are less dramatic, especially for poststack processing of narrow-azimuth, moderate-spread data. Also, incorporating anisotropy into velocity analysis requires estimation of several independent, spatially variable parameters, which may not be constrained by P-wave reflection traveltimes. Hence, the progress in P-wave processing can be largely attributed to breakthroughs in parameterization of transversely isotropic (TI) models, most notably the introduction of Thomsen (1986) notation and the discovery of the P-wave time-processing parameter η (Alkhalifah and Tsvankin, 1995). The exploding interest in anisotropy and the importance of the parameterization issue have

Manuscript received by the Editor 8 December 2009; revised manuscript received 1 February 2010; published online 14 September 2010.
[1]Colorado School of Mines, Department of Geophysics, Center for Wave Phenomena, Golden, Colorado, U.S.A. E-mail: ilya@dix.mines.edu.
[2]Geokinetics, Denver, Colorado, U.S.A. E-mail: jim.gaiser@geokinetics.com.
[3]Shell Exploration & Production Company, Houston, Texas, U.S.A. E-mail: Vladimir.Grechka@Shell.com.
[4]University of Alberta, Department of Physics, Edmonton, Alberta, Canada. E-mail: Mirko.vanderBaan@ualberta.ca.
[5]Delta Geophysics, Houston, Texas, U.S.A. E-mail: leon.thomsen@deltageophysics.net.

made Thomsen's classical 1986 article the top-cited paper ever published in the journal GEOPHYSICS.

More recently, the inadequacy of isotropic velocity models was exposed by the advent of prestack depth migration, which is highly sensitive to the accuracy of the velocity field. As a result, TI models with a vertical (VTI) and tilted (TTI) axis of symmetry have become practically standard in prestack imaging projects all over the world. For instance, anisotropic algorithms produce markedly improved images of subsalt exploration targets in the Gulf of Mexico, which has long been considered as a region with relatively "mild" anisotropy.

The goal of this paper is to give a brief description of the state of the art in anisotropic modeling, processing, and inversion and to outline the main future trends. It is impossible to give a complete picture of the field in a journal article, and the selection of the material inevitably reflects the personal research experience and preferences of the authors. For in-depth discussion of theoretical and applied aspects of seismic anisotropy, we refer the reader to the books by Helbig (1994), Thomsen (2002), Tsvankin (2005), and Grechka (2009).

NOTATION FOR ANISOTROPIC MEDIA

One of the most critical issues in seismic data analysis for anisotropic media is a proper design of model parameterization. Whereas the stiffness coefficients (c_{ij}) are convenient to use in forward-modeling algorithms, they are not well suited for application in seismic processing and inversion. An alternative notation for transverse isotropy was introduced by Thomsen (1986), who suggested to describe the medium by the symmetry-direction velocities of P- and S-waves (V_{P0} and V_{S0}, respectively) and three dimensionless parameters (ε, δ, and γ), which characterize the magnitude of anisotropy. The parameter ε is close to the fractional difference between the P-wave velocities in the directions perpendicular and parallel to the symmetry axis, so it defines what is often simplistically called the "P-wave anisotropy." Likewise, γ represents the same measure for SH-waves. While the definition of δ seems less transparent, this parameter also has a clear meaning — it governs the P-wave velocity variation away from the symmetry axis and also influences the SV-wave velocity.

Although Thomsen originally used the assumption of weak anisotropy (i.e., $|\epsilon| \ll 1$, $|\delta| \ll 1$, and $|\gamma| \ll 1$), his notation has since emerged as the best choice in seismic processing for TI media with *any* magnitude of velocity variations. Indeed, Thomsen parameters capture the combinations of the stiffness coefficients constrained by seismic signatures (for details, see Tsvankin, 2005). In particular, P-wave kinematics for TI media with a given symmetry-axis orientation depend on just three Thomsen parameters (V_{P0}, ε, and δ; the contribution of V_{S0} is negligible), rather than four stiffness coefficients (c_{11}, c_{13}, c_{33}, and c_{55}). Thomsen notation is especially convenient for reflection data processing because it greatly simplifies expressions for normal-moveout (NMO) velocity, quartic moveout coefficient, amplitude-variation-with-offset (AVO) response, and geometric spreading. Linearization of exact equations in ε, δ, and γ provides valuable insight into the influence of transverse isotropy on seismic wavefields and helps guide inversion and processing algorithms.

Moreover, the contribution of anisotropy to time-domain processing of P-wave reflection data for VTI media is absorbed by the single "anellipticity" parameter η close to the difference between ε and δ [$\eta \equiv (\varepsilon - \delta)/(1 + 2\delta)$]. The interval values of η and the NMO velocity for horizontal reflectors [$V_{\rm nmo}(0)$] are sufficient to perform normal-moveout and dip-moveout corrections and prestack and poststack time migration for VTI models with a laterally homogeneous overburden (Alkhalifah and Tsvankin, 1995). Most important, the time-processing parameters $V_{\rm nmo}(0)$ and η can be estimated just from P-wave reflection traveltimes using NMO velocity of dipping events or nonhyperbolic moveout.

The parameters required for P-wave imaging and AVO analysis in VTI media are listed in Table 1. Whereas ϵ usually quantifies the magnitude of P-wave velocity variations, the parameters of more importance in seismic processing are δ and η. Laboratory measurements of the anisotropy parameters for sedimentary rocks from different regions are summarized by Wang (2002). Both rock-physics and seismic data indicate that vertical and tilted transverse isotropy in sedimentary basins are mostly associated with the intrinsic anisotropy of shales caused by aligned plate-shaped clay particles. Many sedimentary formations including sands and carbonates, however, contain vertical or steeply dipping fracture sets and should be described by effective symmetries lower than TI, such as orthorhombic (see below). The effective anisotropy parameters are also influenced by fine layering on a scale small compared to seismic wavelength (Backus, 1962).

The principle of Thomsen notation has been extended to orthorhombic (Tsvankin, 1997, 2005), monoclinic (Grechka et al., 2000), and even the most general, triclinic (Mensch and Rasolofosaon, 1997) models. For instance, Tsvankin's notation for orthorhombic media preserves the attractive features of Thomsen parameters in describing the symmetry-plane velocities, traveltimes, and plane-wave reflection coefficients of P-, S_1-, and S_2-waves. It also reduces the number of parameters responsible for P-wave kinematics and provides a unified framework for treating orthorhombic and TI models in parameter-estimation methods operating with wide-azimuth, multicomponent data (Grechka et al., 2005).

Estimation of anisotropy from P-wave vertical seismic profiling (VSP) data acquired under a structurally complex overburden involves expressing the vertical slowness component in terms of the polarization direction. This problem, discussed in more detail below, leads to the definition of Thomsen-style anisotropy parameters specifically tailored to VSP applications (Grechka and Mateeva, 2007; Grechka et al., 2007).

Furthermore, Thomsen notation has been generalized for *attenuative* TI and orthorhombic media in order to facilitate analytic description and inversion of body-wave attenuation coefficients (Zhu and Tsvankin, 2006, 2007). For a model with VTI symmetry of both the real and imaginary parts of the stiffness matrix, this notation (in addition to the velocity-anisotropy parameters) includes the vertical attenuation coefficients of P- and S-waves ($\mathcal{A}_{P0}$ and $\mathcal{A}_{S0}$) and three dimensionless parameters (ϵ_Q, δ_Q, and γ_Q) responsible for attenua-

Table 1. P-wave parameters for imaging and AVO analysis in VTI media. The parameter $V_{\rm nmo}(0) = V_{P0}\sqrt{1 + 2\delta}$ is the NMO velocity for horizontal reflectors.

Full set	Depth imaging	Time imaging	AVO (intercept, gradient)
V_{P0}	V_{P0}	$V_{\rm nmo}(0)$	V_{P0}
ε or η	ε or η	η	—
δ	δ	—	δ
V_{S0}	—	—	V_{S0}

tion anisotropy. Linearization of the P-wave phase attenuation coefficient in the anisotropy parameters yields an expression that has exactly the same form as Thomsen's (1986) weak-anisotropy approximation for P-wave phase velocity.

Whereas the optimal choice of notation is a prerequisite for successful anisotropic parameter estimation and processing, it is also important in forward modeling, which is discussed next.

FORWARD MODELING OF BODY WAVES

The ability to compute synthetic seismograms has always been a high priority in geophysics since accurate forward modeling can be a valuable aid in seismic interpretation and inversion. Unfortunately, a fully anisotropic (triclinic) earth is characterized by 21 stiffness coefficients (or Thomsen-style parameters) and density, all of which may vary in space.

Full-waveform modeling can be implemented by solving the wave equation for a general 3D (an)elastic medium using numerical techniques such as finite-difference, finite-element, pseudospectral and spectral-element methods (Kosloff and Baysal, 1982; Virieux, 1986; Komatitsch and Tromp, 1999). Although originally many of these approaches were developed for isotropic media, most have been extended to handle anisotropic, anelastic media (Carcione et al., 1988; Komatitsch et al., 2000). For a recent review, see Carcione et al. (2002).

Despite the constantly increasing computational power, full anisotropic (i.e., with 21 stiffnesses) modeling using the above techniques is still rarely attempted due to the scale of the problem and the staggering number of possible models. In practice, three avenues are commonly explored to facilitate interpretation and reduce computation demands: (1) simplifications to theory; (2) reduction of information content in the acquired data; and (3) limitations to considered structures, anisotropic symmetries, and/or medium types. For instance, seismic waves are often represented through rays, thereby invoking a high-frequency approximation (simplifications to theory). Also, one can choose to analyze traveltimes and/or amplitudes only (reduction in information content), treat only specific types of anisotropy, assume that wave motion can be described by P-wave propagation in acoustic media, and/or impose lateral continuity and consider only vertically heterogeneous structures (constraints on media and/or structures). Obviously, several approaches can be combined to develop an appropriate interpretation strategy.

The earliest efforts to compute body-wave synthetics in anisotropic media focused on either simulation of full waveforms for simple models with at most one interface (Buchwald, 1959; Lighthill, 1960) or traveltime calculations by means of geometric ray theory (Vlaar, 1968; Červený, 1972). The former efforts were motivated by the development of ultrasonic techniques for the measurement of dynamic elastic constants of pure crystals and metals (Musgrave, 1970; Auld, 1973). The latter approach was largely directed at explaining and understanding anomalous body-wave properties observed in refraction experiments and seismic arrays (Hess, 1964).

The ray method is a far-field, high-frequency, asymptotic approximation, which can handle laterally and vertically heterogeneous anisotropic media under the assumption that the medium parameters vary smoothly on the scale of wavelength. In addition to being much less computationally intensive than finite-difference schemes and similar numerical methods, ray theory makes it possible to model individual wave types rather than the whole wavefield. While ray tracing can be used to generate both traveltimes and amplitudes, serious difficulties arise (especially for amplitude computations) near singular areas, such as caustics, cusps and conical points on the wavefronts, shadow zones, and propagation directions for which the velocities of the split S-waves are close (Gajewski and Pšenčík, 1987). Some of these problems are related to wavefront folding when many rays pass through a common focal point or focal line — a phenomenon that complicates the evaluation of geometric spreading. Geometric ray theory also excludes head waves. Despite its limitations, ray theory is still at the heart of many migration algorithms that employ ray tracing for efficient generation of traveltime tables. A more detailed discussion of ray theory can be found in the paper by Carcione et al. (2002) and in monographs by Červený (2001) and Chapman (2004).

The reflectivity method takes an alternative avenue to compute full-waveform synthetics in laterally homogeneous media (Kennett, 1983). The technique is based on plane-wave decomposition of point-source radiation combined with the solution of the plane-wave reflection/transmission problem for layered media obtained using so-called propagator matrices (Haskell, 1953; Gilbert and Backus, 1966). It can model both kinematic and dynamic properties of recorded wavefields, including all primary and multiple reflections, conversions, and head waves, as long as the 1D assumption (i.e., the elastic properties vary only with depth) is satisfied (Fuchs and Müller, 1971; Kennett, 1972). The anisotropic reflectivity method, originally developed for VTI models and symmetry-plane wave propagation (Keith and Crampin, 1977; Booth and Crampin, 1983), has been extended to azimuthally anisotropic media (Fryer and Frazer, 1984; Tsvankin and Chesnokov, 1990).

Despite its 1D model assumption, the reflectivity method has proved to be a valuable tool for understanding and interpreting wave-propagation phenomena in both VSP and surface-seismic acquisition geometries. For instance, Mallick and Frazer (1991) employ this technique to study P-wave amplitude variations with offset and azimuth in a medium containing vertical fractures and demonstrate how azimuthal amplitude anomalies can help reveal fracture orientation.

P-WAVE VELOCITY ANALYSIS AND IMAGING

Most isotropic time- and depth-migration algorithms (Kirchhoff, Stolt, phase-shift, phase-shift-plus-interpolation (PSPI), Gaussian beam, finite-difference, etc.) have been generalized for VTI and, in many cases, for TTI media (e.g., Sena and Toksöz, 1993; Anderson et al., 1996; Alkhalifah, 1997; Ren et al., 2005; Zhu et al., 2007a). The key issue in anisotropic processing, however, is reliable estimation of the velocity model from reflection data combined with borehole and other information. The parameter η responsible for time processing in VTI media can be obtained by inverting either dip-dependent NMO velocity or nonhyperbolic (long-spread) reflection moveout (Alkhalifah and Tsvankin, 1995; Alkhalifah, 1997; Toldi et al., 1999; Fomel, 2004; Tsvankin, 2005; Ursin and Stovas, 2006). Then the η-field can be refined in the migrated domain using migration velocity analysis (Sarkar and Tsvankin, 2004) or reflection tomography (Woodward et al., 2008).

Building VTI velocity models in the depth domain typically requires *a priori* constraints because the vertical velocity V_{P0} and the parameters ϵ and δ can seldom be determined from P-wave reflection moveout alone. In many cases, V_{P0} is found from check shots or well logs at borehole locations and is used in combination with the stacking (NMO) velocity to compute the parameter δ. Note that ig-

noring the contribution of δ to NMO velocity in isotropic processing leads to misties in time-to-depth conversion. Then the velocity field can be constructed by interpolating the parameters V_{P0} or δ between the boreholes and estimating η (and, therefore, ϵ) from reflection data. Integration of seismic and borehole data can be facilitated by applying geologic constraints in the process of interpretive model

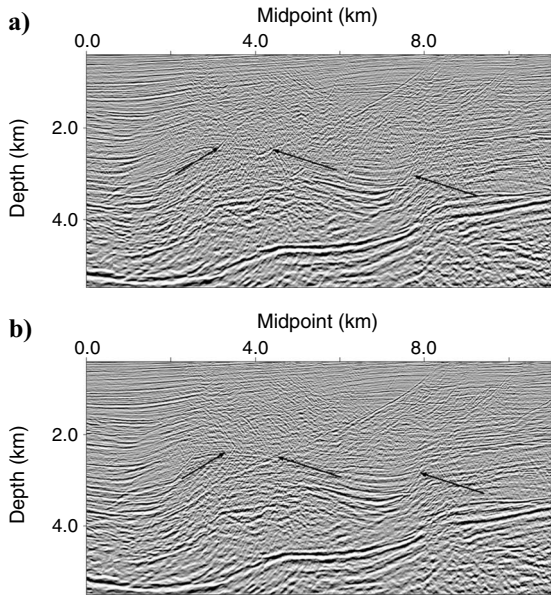

Figure 1. Comparison between isotropic and VTI time imaging (after Alkhalifah et al., 1996, and Sarkar and Tsvankin, 2006). A 2D line from West Africa after (a) isotropic and (b) anisotropic time imaging. The processing sequence included NMO and DMO corrections and poststack phase-shift time migration. Both time sections are stretched to depth. The arrows point to the main improvements achieved by taking anisotropy into account.

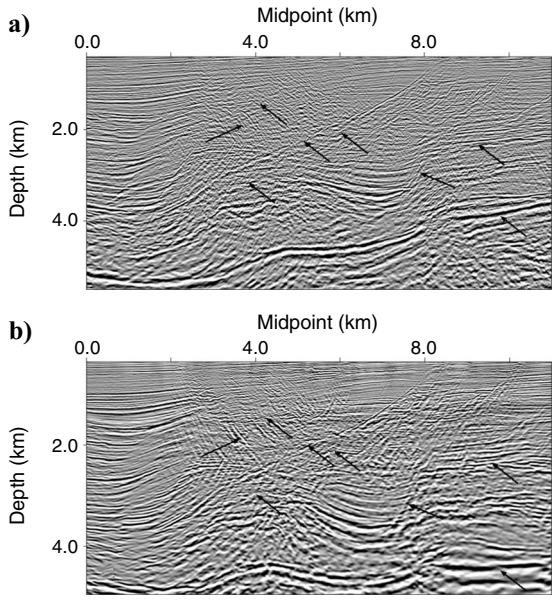

Figure 2. Comparison between VTI time and depth imaging (after Sarkar and Tsvankin, 2006). The line from Figure 1 after (a) anisotropic time processing (same as Figure 1b) and (b) anisotropic MVA and prestack depth migration. The arrows point to the main differences between the two sections.

updating (Bear et al., 2005) or recasting the generation of a dense anisotropic velocity field as an optimization problem. An efficient tool for building heterogeneous VTI models is postmigration grid tomography based on iterative minimization of residual moveout after prestack depth migration (Woodward et al., 2008).

Anisotropic migration with the estimated Thomsen parameters typically produces sections with better focusing and positioning of reflectors for a wide range of dips, including steep interfaces such as flanks of salt domes. The 2D line in Figure 1 is used by Alkhalifah et al. (1996) to illustrate the improvements achieved by anisotropic time processing in offshore West Africa where thick TI shale formations cause serious imaging problems (Ball, 1995). For example, VTI dip-moveout and poststack migration algorithms succeeded in imaging the fault plane at midpoint 7.5 km and depth 3 km (the right arrow in Figure 1b), which is absent on the isotropic section (Figure 1a). Also, the major fault plane between the midpoints at 2 km and 8 km (it stretches up and down from the middle arrow in Figure 1a and b) and gently dipping reflectors throughout the section appear more crisp and continuous. Accurate fault imaging beneath the shales plays a major role in prospect identification in the area.

It is even more critical to properly account for anisotropy in prestack depth migration because the results of prestack imaging are highly sensitive to the quality of the velocity model. The section in Figure 2b was produced by applying VTI migration velocity analysis (MVA) and Kirchhoff prestack depth migration to the line from Figure 1 (Sarkar and Tsvankin, 2006). MVA was carried out by dividing the section into factorized VTI blocks, in which the parameters ϵ and δ are constant, while the velocity V_{P0} is a linear function of the spatial coordinates. Factorized VTI is the simplest model that allows for both anisotropy and heterogeneity and requires minimal *a priori* information to constrain the relevant parameters (Sarkar and Tsvankin, 2004). In the absence of pronounced velocity jumps across layer boundaries, knowledge of the vertical velocity at the top of a piecewise-factorized VTI medium is sufficient to estimate the parameters V_{P0}, ϵ, and δ along with the velocity gradients throughout the section using only P-wave data (Figure 3a, c, and d).

The velocity analysis revealed significant lateral velocity gradients in some of the layers (Figure 3a), which could not be handled by

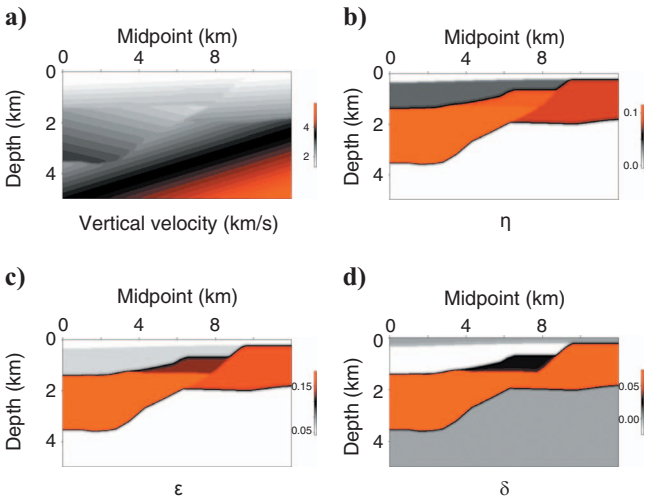

Figure 3. Estimated parameters (a) V_{P0}, (b) η, (c) ε, and (d) δ used to generate the depth-migrated section in Figure 2b (after Sarkar and Tsvankin, 2006).

time-domain techniques. As a result, the depth-domain parameter estimation produced a more reliable, laterally varying η-field (Figure 3b). The depth imaging facilitated structural interpretation of the deeper part of the section by removing the false dips seen in Figure 2a. Also, most antithetic faults that look fuzzy on the time section are well focused, and subhorizontal reflectors within the anisotropic layers are better positioned and stacked. This and many other published case studies demonstrate that a major advantage of anisotropic depth imaging is in providing accurate well ties without sacrificing image quality.

In tectonically active areas or in the presence of dipping fracture sets, the symmetry axis of TI formations can be tilted, and the VTI model becomes inadequate. Tilted transverse isotropy is common in the Canadian Foothills, where shale layers are often bent and may have steep, variable dips (e.g., Vestrum et al., 1999). Also, uptilted shale layers near salt domes may cause serious difficulties in imaging steeply dipping segments of the salt flanks (Tsvankin, 2005). A detailed description of distortions caused by applying VTI algorithms to data from typical TTI media can be found in Behera and Tsvankin (2009), who extend MVA to TI models with the symmetry axis orthogonal to reflectors. In their case studies from the Gulf of Mexico, Huang et al. (2009) and Neal et al. (2009) demonstrate that accounting for the tilt of the symmetry axis produces significant improvements in imaging of steep dips, fault resolution, and spatial positioning of reflectors. The inadequacy of VTI models for many subsalt plays in the Gulf of Mexico has become especially apparent with acquisition of wide-azimuth surveys. In complicated structural environments, the full benefits of TI imaging can be realized with reverse time migration (RTM) based on solving the two-way wave equation (Huang et al., 2009). RTM with TTI or VTI velocity models is already widely used in GoM subsalt imaging projects.

Despite the recent successes, parameter estimation for heterogeneous TTI media remains a highly challenging problem, even with the common assumption that the symmetry axis is orthogonal to reflectors. Methods currently under development combine TI ray-based reflection tomography with check shots and walkaway VSP surveys (e.g., Bakulin et al., 2009). It is likely that processing of high-quality wide-azimuth surveys in some areas will require employing more complicated (but more realistic), orthorhombic velocity models. A promising direction for high-resolution anisotropic velocity analysis is full-waveform inversion, which so far has been developed mostly for acoustic models.

SLOWNESS-BASED PROCESSING AND INVERSION

Processing and inversion of surface seismic data are mostly done in the time-offset domain, yet other domains may offer advantages in terms of noise suppression and/or inversion for anisotropy parameters. It is especially beneficial to transform seismic data into the slowness domain, with applications as diverse as common-conversion-point sorting, anisotropy estimation, geometric-spreading correction, and amplitude and full-waveform inversion.

Snell's law states that the horizontal slowness p does not change along a ray in 1D models. This fact helps identify correlated pure-mode (PP) and converted (PS) reflections from the same interface that have common downgoing P-wave ray segments (and therefore the same horizontal slownesses). Identification of common ray segments leads to a straightforward common-conversion-point sorting scheme in both the time-offset and intercept time–horizontal slowness (τ-p) domains (van der Baan, 2005). In the presence of lateral and vertical velocity variations, one can still identify PP and PS reflections with the same takeoff angles (i.e., the same horizontal slownesses) at the source by matching their time slopes in common-receiver gathers. This more general scheme, called "PP + PS = SS" (discussed in more detail below), is designed to construct the traveltimes of pure-mode SS reflections solely from acquired PP- and PS-waves (Grechka and Tsvankin, 2002).

Slowness-based traveltime inversion can also increase the accuracy of interval parameter estimation. Anisotropic traveltime inversion is often based on moveout approximations that become unnecessary if seismic data are processed by means of a plane-wave decomposition, such as the τ-p transform. Indeed, plane-wave propagation is directly governed by phase rather than group velocities because the interval $\tau(p)$ curves represent rescaled versions of the slowness functions (Hake, 1986). Note that phase velocities generally are less complex mathematically compared to group velocities.

A τ-p domain approach has been applied by Gaiser (1990) to analysis of VSP data, by Hake (1986) and van der Baan and Kendall (2002, 2003) to inversion of reflections traveltimes, and by Mah and Schmitt (2003) to processing of ultrasonic measurements. Similar gains in accuracy can be obtained by formulating slowness-based inversion algorithms directly in the time-offset domain (Douma and van der Baan, 2008; Fowler et al., 2008; Dewangan and Tsvankin, 2006a; Wang and Tsvankin, 2009). It should be mentioned that the velocity-independent layer-stripping method of Dewangan and Tsvankin (2006a) is valid for an arbitrarily heterogeneous target horizon. An important feature of slowness-based algorithms is that they replace Dix-type differentiation of moveout parameters with traveltime stripping (Figure 4), which increases the accuracy and stability of interval parameter estimates.

Plane-wave decomposition also represents a convenient tool for geometric-spreading correction in horizontally layered media. Indeed, plane waves in 1D models are not subject to geometric spreading (in contrast to spherical waves); this is implicitly used in the reflectivity method discussed above (Fuchs and Müller, 1971; Kennett, 1983; Fryer and Frazer, 1984). Wang and McCowan (1989), Dunne and Beresford (1998), and van der Baan (2004) explicitly

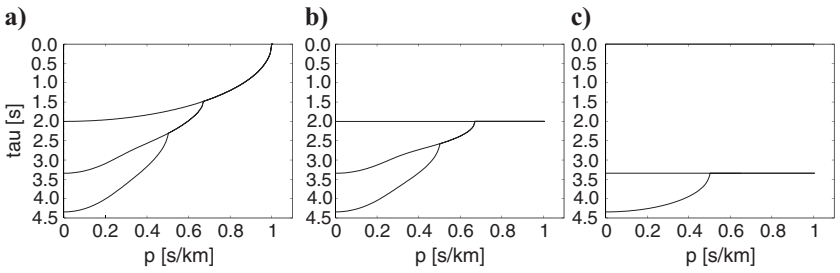

Figure 4. Layer stripping in the τ-p domain (after van der Baan and Kendall, 2002). A hyperbolic moveout curve in the time-offset domain maps onto an ellipse in the τ-p domain, and nonhyperbolic moveout manifests itself by a deviation from the ellipse. (a) Moveout curves in the τ-p domain are created by summing the contributions of the individual layers. Removing the influence of (b) the top layer or (c) the two top layers yields the moveout in the corresponding interval. The first and third layers are isotropic, whereas the second layer is anisotropic, as evidenced by the strong deviation of its interval moveout from an ellipse on plot (b).

employ plane-wave decomposition to remove the geometric-spreading factor from the amplitudes of all primary and multiple reflections (including mode conversions) simultaneously. Subsequent moveout correction and stacking in the τ-p domain (Stoffa et al., 1981, 1982) generates higher-quality stacked sections compared to those produced by the standard time-offset stacking process (Figure 5). Interestingly, stacking in the slowness domain preserves head waves suppressed by conventional processing (van der Baan, 2004).

Finally, plane-wave decomposition may facilitate amplitude analysis at far offsets near and beyond the critical angle, where the wavefield in the time-offset domain cannot be described by plane-wave reflection coefficients (van der Baan, 2004; van der Baan and Smit, 2006; Tsvankin, 1995a). Thus, slowness-based processing and inversion have many advantages for data from anisotropic media. Indeed, it has been suggested in the literature that seismic inversion techniques should be applied to slant-stacked data obtained after a plane-wave decomposition (Müller, 1971; Fryer, 1980; Treitel et al., 1982). This approach is also suitable for full-waveform inversion in stratified media (Kormendi and Dietrich, 1991; Martinez and McMechan, 1991; Ji and Singh, 2005) and separation of interfering PP and PS waves (van der Baan, 2006).

ANISOTROPY ESTIMATION FROM VSP DATA

The concept of operating with slowness measurements is also essential in processing of vertical seismic profiling surveys. Although anisotropic velocity models have to be built based on surface reflection data for most applications in seismic exploration, VSP can often provide useful complementary anisotropy estimates. Because those estimates are made at seismic frequencies, they have an important advantage over well-log anisotropy measurements, which pertain to the frequency range of 10^3–10^4 Hz and require upscaling for use in seismic processing. The anisotropy parameters constrained by VSP data strongly depend on both the acquisition design and the magnitude of lateral heterogeneity of the overburden.

The simplest VSP experiment involves a single geophone placed in a well. First-break P-wave times picked from such VSP data reflect the influence of effective anisotropy between the earth's surface, where the seismic sources are located, and the geophone's depth. Because this depth is known, P-wave walkaway VSP data (or the combination of surface reflection data and check shots) for laterally homogeneous VTI media yield the effective Thomsen parameter δ. Whether or not it is possible to estimate another anisotropy parameter (η or ϵ) governing P-wave kinematics depends on the presence of sufficiently large offsets in the data. While the usefulness of such low-resolution anisotropy estimates might be questioned, P-wave traveltimes recorded in any VSP geometry help build an exact depth-migration operator suitable for constructing a subsurface image near the geophone.

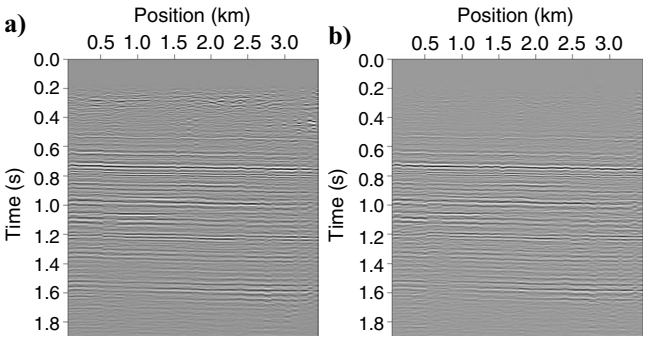

Figure 5. Comparison of stacking techniques on field data (after van der Baan, 2004). (a) A conventional t-x stacked section after the geometric-spreading correction. (b) The same section obtained by stacking in the τ-p domain after applying plane-wave decomposition to remove geometric spreading. The two sections are structurally similar but τ-p processing produced a higher signal-to-noise ratio at small traveltimes and somewhat different reflector amplitudes between 1.3 s and 1.6 s.

The opposite "end member" is a wide-azimuth, multicomponent VSP survey recorded by a string of geophones placed beneath a laterally homogeneous overburden. Such VSP data make it possible to obtain a complete (triclinic) local stiffness tensor near the borehole. This is demonstrated by Dewangan and Grechka (2003) who apply the so-called slowness-polarization method (White et al., 1983; de Parscau, 1991; Hsu et al., 1991; Horne and Leaney, 2000) to estimate anisotropy from the traveltimes and polarization directions of P-, S_1-, and S_2-waves recorded at Vacuum field (New Mexico, USA). They conclude that the VSP measurements can be well-described by an orthorhombic model with a near-horizontal symmetry plane. Unfortunately, the slowness-polarization method can be successfully implemented only when lateral heterogeneity of the overburden is negligible. Then the horizontal slowness components, which are measured on common-receiver gathers and pertain to seismic sources at the earth's surface, can be used to reconstruct the slowness surface at geophone locations (Gaiser, 1990; Miller and Spencer, 1994; Jílek et al., 2003).

Strong lateral heterogeneity (for instance, due to the presence of salt in the overburden) renders reconstruction of the slowness surfaces inaccurate and often makes shear-wave arrivals too noisy for anisotropic inversion. Consequently, anisotropy has to be inferred from P-waves only, which leads to the introduction of Thomsen-style parameters for P-wave VSP inversion. The measured quantities include the P-wave vertical slowness component, q, expressed as a function of the polar (ψ) and azimuthal (φ) angles of the polarization vector. The values of q, ψ, and φ do not depend on the structural complexity of the overburden and correspond to the vicinity (with the spatial extent approximately equal to the wavelength) of downhole geophones. If the medium around the borehole is VTI, the vertical slowness q is independent of the polarization azimuth φ, and the weak-anisotropy approximation for $q(\psi)$ takes the form (Grechka and Mateeva, 2007)

$$q(\psi) = \frac{\cos\psi}{V_{P0}}(1 + \delta_{\mathrm{VSP}} \sin^2\psi + \eta_{\mathrm{VSP}} \sin^4\psi), \qquad (1)$$

where

$$\delta_{\mathrm{VSP}} = \frac{\delta}{(V_{P0}/V_{S0})^2 - 1} \quad \text{and} \quad \eta_{\mathrm{VSP}} = \eta\,\frac{(V_{P0}/V_{S0})^2 + 1}{(V_{P0}/V_{S0})^2 - 1} \qquad (2)$$

are the anisotropy parameters responsible for the P-wave slowness-of-polarization dependence.

The pairs $\{\delta_{\mathrm{VSP}}, \eta_{\mathrm{VSP}}\}$ and $\{\delta, \eta\}$ play comparable roles for processing of P-wave VSPs acquired along vertical boreholes and of P-wave surface reflection data, respectively, in VTI media. Indeed, equation 1 reveals that δ_{VSP} is responsible for the near-vertical variation of $q(\psi)$, while η_{VSP} governs the vertical slowness at larger polarization angles. Importantly, δ_{VSP} and η_{VSP} absorb the shear-wave

velocity V_{S0}, rendering its value unnecessary for fitting the P-wave slowness-of-polarization functions. Grechka and Mateeva (2007) illustrate this point and present estimates of δ_{VSP} and η_{VSP} in a salt body and subsalt sediments in the deepwater Gulf of Mexico. Whereas the salt proved to be nearly isotropic, δ_{VSP} in the subsalt sediments exhibits a clear correlation with lithology (Figure 6). As is usually the case for the parameter δ, the value of δ_{VSP} is larger in shales than in a predominantly sandy interval.

This technique of anisotropy estimation from P-wave VSP surveys has been extended to azimuthal anisotropy. For example, Grechka et al. (2007) invert wide-azimuth VSP data acquired at tight-gas Rulison field (Colorado, USA) for Tsvankin's (1997) parameters of orthorhombic media and show that the estimated anisotropic model is consistent with the presence of gas-filled vertical fractures in a VTI host rock.

AZIMUTHAL MOVEOUT ANALYSIS

Azimuthal variation of traveltimes, amplitudes, and attenuation coefficients of reflected waves can provide valuable information about anisotropy associated with natural fracture systems, nonhydrostatic stresses, or dipping TI layers (e.g., Lynn et al., 1999; Rüger, 2002). Wide-azimuth P-wave data are often acquired on land for purposes of fracture characterization via azimuthal moveout and AVO analysis. The rapid advent of wide-azimuth offshore technology, designed primarily for better imaging of subsalt exploration targets, is expected to further stimulate development of processing algorithms for azimuthally anisotropic models.

Moveout analysis of wide-azimuth, conventional-spread data is based on the concept of the NMO ellipse and on the generalized Dix-type averaging equations (Grechka and Tsvankin, 1998; Grechka et al., 1999). The normal-moveout velocity of pure (nonconverted) reflected waves expressed as a function of the azimuth α of the CMP line is given by the following quadratic form:

$$V_{nmo}^{-2}(\alpha) = W_{11}\cos^2\alpha + 2W_{12}\sin\alpha\cos\alpha + W_{22}\sin^2\alpha, \quad (3)$$

where $\mathbf{W}$ is a symmetric 2×2 matrix determined by the medium properties around the zero-offset ray. If the traveltime increases with offset in all azimuthal directions (i.e., in the absence of reverse moveout), $V_{nmo}(\alpha)$ traces out an *ellipse*, even for arbitrarily anisotropic, heterogeneous media. Furthermore, equation 3 can be applied to mode-converted waves, if their moveout in CMP geometry is symmetric with respect to zero offset (this is the case for horizontally layered models with a horizontal symmetry plane).

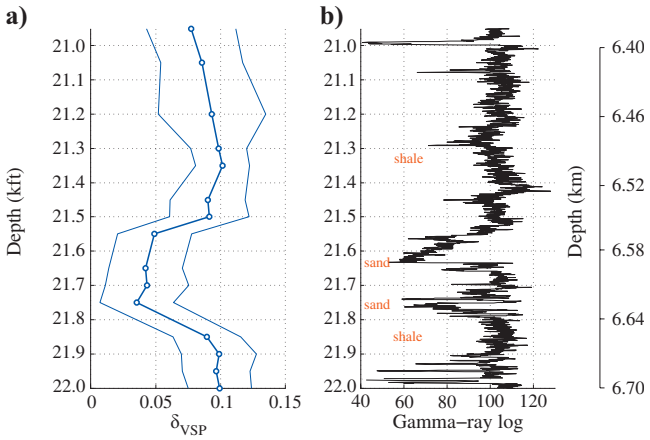

Figure 6. Comparison of (a) the anisotropy parameter δ_{VSP} (bold line) estimated from VSP for subsalt sediments in the Gulf of Mexico with (b) a gamma-ray log (after Grechka and Mateeva, 2007). The thin lines on plot (a) mark the standard deviation of δ_{VSP}.

The equation of the NMO ellipse provides a simple way to correct for the azimuthal variation in stacking velocity often ignored in conventional processing. Even more importantly, the semiaxes and orientation of the NMO ellipse can be used in anisotropic parameter estimation and fracture characterization. A critical issue in moveout analysis of wide-azimuth data is separation of the influence of anisotropy and lateral heterogeneity (in the form of velocity gradients, dipping interfaces, velocity lenses, etc.) on reflection traveltimes (e.g., Jenner, 2009). A data-driven correction of the NMO ellipse for lateral velocity variation in horizontally layered media is suggested by Grechka and Tsvankin (1999), who present a complete processing sequence for azimuthal moveout inversion that also includes 3D "global" semblance analysis and generalized Dix differentiation of effective NMO ellipses. They show that the orientation of the P-wave interval NMO ellipses produced by this methodology in the Powder River Basin (Wyoming, USA) is well-correlated with the depth-varying fracture trends in the field.

P-wave azimuthal moveout analysis has proved to be effective in predicting the dominant fracture orientation in many other exploration regions (e.g., Corrigan et al., 1996; Lynn et al., 1999; Tod et al., 2007). Jenner (2001), who has developed a trace-correlation approach for estimating the NMO ellipse, shows that the fast NMO-velocity direction at Weyburn field in Canada is aligned with the dominant fracture strike and the polarization vector of the fast S-wave; this implies that the medium symmetry is HTI or orthorhombic. Still, in some cases the NMO ellipse is rotated with respect to the shear-wave polarization directions, which may indicate the presence of lower symmetries.

Since the P-wave NMO ellipse constrains only three combinations of the medium parameters, its inversion for the physical properties of fractures (e.g., fracture compliances) suffers from ambiguity, which can be reduced by using the NMO ellipses of the split S-waves, nonhyperbolic moveout, or other (amplitude, borehole) information. For instance, joint inversion of the NMO ellipses of P- and S-waves with *a priori* constraints helps build even orthorhombic and monoclinic velocity models (Grechka et al., 2000; Vasconcelos and Grechka, 2007); more details are given in the section on fracture characterization.

Among the first to recognize the benefits of employing nonhyperbolic (long-spread) reflection moveout in anisotropic parameter estimation was Sena (1991), whose analytic traveltime expressions for multilayered, weakly anisotropic media are based upon the "skewed" hyperbolic moveout formulation of Byun et al. (1989). Long-spread, wide-azimuth P-wave traveltime in azimuthally anisotropic media can be accurately described by generalizing the nonhyperbolic moveout equations of Tsvankin and Thomsen (1994) and Alkhalifah and Tsvankin (1995) originally designed for VTI media. Vasconcelos and Tsvankin (2006) develop a moveout-inversion algorithm for horizontally layered orthorhombic media based on the extended Alkhalifah-Tsvankin equation:

$$t^2(x,\alpha) = t_0^2 + \frac{x^2}{V_{\rm nmo}^2(\alpha)} - \frac{2\eta(\alpha)x^4}{V_{\rm nmo}^2(\alpha)[t_0^2 V_{\rm nmo}^2(\alpha) + (1+2\eta(\alpha))x^2]}, \quad (4)$$

where t_0 is the zero-offset time, $V_{\rm nmo}(\alpha)$ is the NMO ellipse (equation 3), and $\eta(\alpha)$ is the azimuthally varying anellipticity parameter. Equation 4 can be combined with the velocity-independent layer-stripping method (Dewangan and Tsvankin, 2006a) to compute the interval traveltime in the target layer and estimate the interval NMO ellipse and anellipticity parameters $\eta^{(1)}$, $\eta^{(2)}$, and $\eta^{(3)}$ (Wang and Tsvankin, 2009). Nonhyperbolic moveout inversion of wide-azimuth data not only represents a promising fracture-characterization technique (see the case study in Vasconcelos and Tsvankin, 2006), but also provides the input parameters for P-wave time imaging and geometric-spreading correction in layered orthorhombic media.

PRESTACK AMPLITUDE ANALYSIS

Angle-dependent reflection and transmission coefficients contain valuable information about the local medium properties on both sides of an interface. Therefore, analysis of amplitude variations with incidence angle (usually called AVO — amplitude variation with offset) and/or azimuth is often used in reservoir characterization. Because reflection coefficients are determined by the elastic properties averaged on the scale of seismic wavelength, AVO analysis can achieve a much higher vertical resolution than traveltime methods.

Exact equations for plane-wave reflection coefficients are cumbersome even for isotropy and, therefore, rarely used in processing. Whereas exact reflection coefficients for VTI media and symmetry planes of orthorhombic media can still be obtained in closed form (Daley and Hron, 1977; Rüger, 2002), for lower symmetries it is necessary to apply computational schemes (e.g., Fryer and Frazer, 1984; Jílek, 2002a, b). Important insight into anisotropic reflectivity is provided by linearized weak-contrast, weak-anisotropy approximations, which have a much simpler form and often reduce the number of free parameters. The approximate P-wave reflection coefficient for VTI media depends on the contrasts in the vertical P- and S-wave velocities (V_{P0} and V_{S0}), density, and the parameters δ and ϵ (Banik, 1987; Thomsen, 1993; Rüger, 1997). Although the contribution of δ distorts the AVO gradient, the P-wave AVO signatures in isotropic and VTI media are generally similar, which complicates amplitude inversion for the five independent parameters. Indeed, as shown by de Nicolao et al. (1993), only two parameters can be resolved from the isotropic reflection coefficient.

Analysis of azimuthal amplitude variations shows considerably more promise, in particular for estimation of dominant fracture directions in naturally fractured (e.g., tight-gas and tight-oil) reservoirs (Mallick and Frazer, 1991; Gray et al., 2002). Linearized P-wave reflection coefficients were derived for HTI media and symmetry planes of orthorhombic media by Rüger (1997, 1998) and for arbitrary anisotropy by Vavryčuk and Pšenčík (1998); for details, see Rüger's (2002) comprehensive monograph. Application of these analytic expressions in quantitative AVO inversion, however, is hindered by nonuniqueness in parameter estimation. Instead, it is more common to reconstruct the azimuthal variation (which is close to elliptical) of the magnitude of the AVO gradient (Gray et al., 2002; Hall and Kendall, 2003). For HTI and orthorhombic media, the extrema of the AVO gradient lie in the orthogonal vertical symmetry planes of the model.

If azimuthal anisotropy is caused by one set of vertical fractures, the maximum AVO gradient may be either parallel or perpendicular to the fractures, which generally leads to a 90°-uncertainty in the fracture azimuth. Despite this ambiguity, the azimuthally varying P-wave AVO response has been successfully used for estimating the dominant fracture orientation and, in some cases, mapping "sweet spots" of intense fracturing (e.g., Gray et al., 2002; Gray and Todorovic-Marinic, 2004; Xu and Tsvankin, 2007). For instance, Hall and Kendall (2003) demonstrate that the direction of the minimum AVO gradient at Valhall field is well-aligned with faults inferred from coherency analysis (Figure 7).

For HTI and orthorhombic media with a single fracture set, the difference between the symmetry-plane AVO gradients is proportional to the fracture density (which is close to the shear-wave splitting parameter) and also depends on the fracture infill (Rüger, 2002). Therefore, even for such simple models the inversion of the P-wave AVO gradient for the fracture properties is generally nonunique. In principle, fracture density and saturation can be constrained by combining the P-wave AVO response and NMO ellipse, but this approach is applicable only to relatively thick, weakly heterogeneous reservoirs (e.g., see Xu and Tsvankin, 2007). Additional complications may be caused by multiple fracture sets (which lower the symmetry to at least orthorhombic) and the presence of fractures on both sides of the target reflector. For such realistic fractured reservoirs, it is highly beneficial to employ multicomponent data in azimuthal AVO analysis (Bakulin et al., 2000; Jílek, 2002a, b; DeVault et al., 2002). In particular, Jílek (2002b) presents a methodology for joint nonlinear AVO inversion of wide-azimuth PP and PS reflections for TI and orthorhombic media.

Another interesting possibility is to combine azimuthal AVO and attenuation analysis, which helps remove the uncertainty in estimating the fracture orientation for HTI media (Clark et al., 2009). Furthermore, body-wave attenuation coefficents are highly sensitive to anisotropy and fracturing and may potentially provide powerful

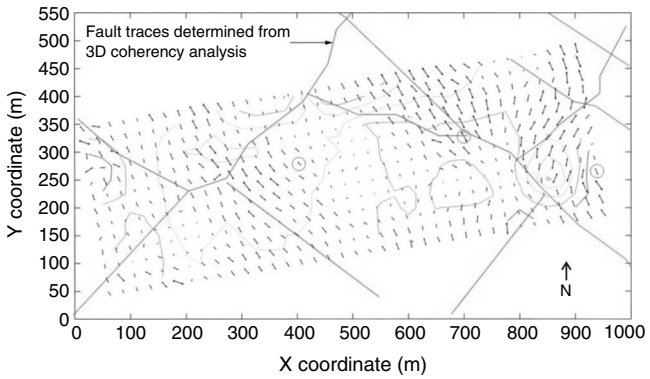

Figure 7. Application of P-wave azimuthal AVO analysis to fracture detection at Valhall field (after Hall and Kendall, 2003). The fracture azimuths (ticks) estimated from the azimuthally varying AVO gradient for the top-chalk horizon are compared with interpreted fault traces. Note the general alignment of fractures with large-scale faulting, especially near the faults trending from northwest to southeast. In the southeast corner, fractures also appear to be perpendicular to the surface curvature defined by the time contours (the contours are plotted at 20-ms intervals, with the red color indicating deeper areas).

fracture-characterization attributes (Chapman, 2003; Zhu et al., 2007b; Chichinina et al., 2009; Maultzsch et al., 2009). On the other hand, in some cases azimuthally varying attenuation (if unaccounted for) may distort the AVO signature. Efficient velocity-independent techniques for estimating interval offset- and azimuth-dependent attenuation from frequency-domain reflection amplitudes are suggested by Behura and Tsvankin (2009) and Reine et al. (2009).

AVO analysis is designed to operate with the plane-wave reflection coefficient at the target interface. The recorded amplitude of reflected waves, however, also depends on the source/receiver directivity and such propagation factors as geometric spreading, transmission coefficients, and attenuation (Martinez, 1993; Maultzsch et al., 2003). Anisotropic layers in the overburden focus or defocus seismic energy like an optical lens, thus distorting the amplitude distribution along the wavefront and causing pronounced angle variations of geometric spreading (Tsvankin, 1995b, 2005; Stovas and Ursin, 2009). In that case, robust reconstruction of the angle-dependent reflection coefficient requires an anisotropic geometric-spreading correction.

Geometric spreading in the time-offset domain is related to the convergence or divergence of ray beams (Gajewski and Pšenčík, 1987) and, therefore, can be computed directly from the spatial derivatives of traveltime (Vanelle and Gajewski, 2003). This ray-theory result is exploited in the moveout-based geometric-spreading correction devised for horizontally layered VTI models by Ursin and Hokstad (2003) and extended to wide-azimuth, long-spread PP and PS data from azimuthally anisotropic media by Xu and Tsvankin (2006, 2008). In particular, this correction has proved to be essential in azimuthal AVO analysis of reflections from the bottom of relatively thick fractured reservoirs (Xu and Tsvankin, 2007).

On the whole, recent developments have laid the groundwork for transforming anisotropic AVO analysis into a valuable reservoir-characterization tool.

PROCESSING AND APPLICATIONS OF MULTICOMPONENT DATA

Early applications of shear-wave seismology had to cope with erratic and unpredictable data quality and misties between SS-wave reflections at the intersection of 2D acquisition lines (Lynn and Thomsen, 1986; Willis et al., 1986). This caused serious difficulties in generating interpretable shear-wave sections and using multicomponent data in lithology discrimination and fracture characterization. Alford (1986) suggested that these problems are related to shear-wave splitting due to azimuthal anisotropy and proposed simple rotation operators to transform SS data into two principal sections containing the fast and slow modes. Likewise, Martin and Davis (1987) discuss the need to rotate converted PS-waves acquired for fracture-characterization purposes at Silo field (Colorado, USA).

Shear waves in anisotropic media exhibit birefringence (shear-wave splitting) and travel as two separate modes with different velocities and orthogonal (for the same phase direction) polarizations. If the medium is HTI or orthorhombic with a horizontal symmetry plane, the vertically traveling split S-waves are polarized in the symmetry planes of the model. The magnitude of shear-wave splitting at vertical incidence is described by the parameter $\gamma^{(S)}$, which is close to the fractional difference between the velocities of the fast (S_1) and slow (S_2) modes and can be estimated as $\gamma^{(S)} \approx (t_s - t_f)/t_f$, where t_s and t_f are the traveltimes of the waves S_2 and S_1, respectively. After separating the split shear waves on prestack data, it may be possible to evaluate their NMO ellipses and AVO signatures.

Pure-mode SS-waves

Processing surface shear-wave data for azimuthal anisotropy analysis has primarily involved 1D compensation for splitting at near-vertical propagation directions. Alford's (1986) rotation algorithm operates on four-component, stacked (supposed to be equivalent to zero-offset) data excited by two orthogonal sources and recorded by two orthogonal receivers. Data can be acquired on a 2D line, with sources and receivers oriented parallel (inline) and perpendicular (crossline) to the acquisition azimuth. The four recorded S-wave displacement components can be represented in the form of the following 2×2 matrix:

$$\mathbf{D} = \begin{pmatrix} D_{XX} & D_{XY} \\ D_{YX} & D_{YY} \end{pmatrix}, \tag{5}$$

where X denotes inline and Y crossline; the first letter in the subscript refers to the source orientation, and the second letter to the receiver orientation. Prestack shear-wave data depend on the anisotropic velocity field and have polarization properties controlled by the azimuth of the line with respect to the symmetry planes. However, stacking or performing AVO inversion of 4C data can provide an estimate of the difference between the normal-incidence reflection coefficients (i.e., AVO intercepts) of the split S-waves, which is governed by the parameter $\gamma^{(S)}$ regardless of the original propagation azimuth.

Thus, even for 2D acquisition geometry, pure shear modes can yield information about azimuthal anisotropy. When the acquisition line is parallel to a vertical symmetry plane and the medium is laterally homogeneous, no reflection energy should be present on the off-diagonal components in equation 5. Out-of-plane (obliquely oriented) lines, however, may contain significant coherent energy on D_{XY} and D_{YX}. Alford's (1986) 4C operator simultaneously rotates the sources and receivers in order to estimate the symmetry-plane azimuths and traveltime difference between the fast and slow S-waves:

$$\mathbf{D}' = \mathbf{R}_S \mathbf{D} \mathbf{R}_R^T, \tag{6}$$

where $\mathbf{R}$ is a 2×2 matrix of rotation around the vertical axis for sources ($\mathbf{R}_S$) and receivers ($\mathbf{R}_R$), and T denotes transpose. Rotation is applied to each CDP consisting of a 4C group of traces. For a certain rotation angle that corresponds to the minimum energy on the off-diagonal components D'_{XY} and D'_{YX}, the data appear as if they were acquired in one of the symmetry planes. This means that the diagonal components, D'_{XX} and D'_{YY}, correspond to the fast and slow shear waves and can be processed to estimate the splitting coefficient.

The 4C rotation dramatically improves the quality of shear-wave reflection data and makes them suitable for lithology discrimination (Alford, 1986). By combining Alford rotation of VSP data with layer stripping, Winterstein and Meadows (1991) evaluate S-wave splitting related to in-situ stress and fractures at Cymric and Railroad Gap oil fields (California, USA). Whereas Alford's method assumes the principal anisotropy directions (i.e., the azimuths of the symmetry planes) to be invariant with depth, Winterstein and Meadows (1991) identify well-resolved, abrupt changes in the principal azimuths and splitting coefficient at several depth levels that could be important for reservoir characterization. Thomsen et al. (1999) ex-

tend the layer-stripping technique to reflected S-waves and discuss the analytic basis for separating the split shear modes on both 4C and 2C (single-source) data.

There have been numerous successful applications of shear-wave splitting for purposes of fracture characterization (e.g., Mueller, 1991; Crampin, 2003; Vasconcelos and Grechka, 2007). Traveltime and amplitude differences between the fast and slow shear waves, as well as their NMO ellipses, can help estimate fracture orientation, density and, in some cases, make inferences about fluid saturation. Also, Angerer et al. (2000) show that shear-wave splitting is a more sensitive time-lapse (4D) indicator of pressure changes in response to CO_2 injection than are P-wave velocities. Their synthetic seismograms based on the anisotropic poroelastic theory of Zatsepin and Crampin (1997) match stacked data before and after injection. Terrell et al. (2002) arrive at similar conclusions in their time-lapse study of CO_2 flood at Weyburn Field in Canada. There is little doubt that moveout and amplitude inversion of multicomponent, multiazimuth data offers the best hope of estimating the anisotropy parameters of subsurface formations.

Mode-converted PS-waves

The majority of multicomponent surveys is acquired without shear-wave sources, so the reflected wavefield is largely composed of compressional waves and mode-converted PS-waves. The most prominent P-to-S conversion typically happens at the reflector; such PS events are sometimes called "C-waves" (Thomsen, 1999). For horizontally layered, azimuthally isotropic media converted PS-waves are polarized in the incidence (sagittal) plane (i.e., they result from P-to-SV conversion). However, if the incident P-wave propagates outside vertical symmetry planes of azimuthally anisotropic media, the reflected PS-wave splits into the fast (PS_1) and slow (PS_2) modes, neither of which is generally polarized in the sagittal plane (e.g., Jílek, 2002a).

An important processing step for mode conversions in the presence of azimuthal anisotropy is rotation of receiver directions from an acquisition coordinate system to a source-centered, radial and transverse coordinate system (Gaiser, 1999). This procedure reveals azimuthal traveltime variations of PS_1- and PS_2-waves on the stacked radial components, as well as polarity reversals in the principal anisotropy directions on the stacked transverse components (Li and MacBeth, 1999).

Similar to pure-mode SS reflections, the fast and slow PS-waves have to be separated for further processing. The feasibility of PS-wave splitting analysis is demonstrated by Garotta and Granger (1988) who analyze the amplitude ratios of the transverse and radial components and apply 2C rotation and layer stripping. Gaiser (1997) shows that Alford rotation and layer stripping (a method similar to that of Winterstein and Meadows, 1991), are applicable to PS-waves in reverse VSP geometry. His technique operates with 4C data from equation 5 where the two rows correspond to source-receiver azimuths 90° apart. The principle of Alford rotation is extended to wide-azimuth PS-wave surveys by Dellinger et al. (2002) who replace stacking of PS_1 and PS_2 reflections with an appropriately designed tensor migration. Their results from Valhall field are mixed, which suggests that azimuthal and lateral velocity variations may seriously complicate PS-wave processing. Recently there has been renewed interest in developing a more formal inversion approach to the PS-wave layer-stripping problem where the objective function is formulated in terms of the PS_1-wave polarization azimuth and the traveltime difference between the split PS-waves (e.g., Bale et al., 2009; Haacke et al., 2009; Simmons, 2009).

In addition to such well-documented applications as imaging beneath gas clouds and lithology discrimination, mode-converted data provide valuable attributes for fracture/stress characterization (Gaiser, 2000). After performing layer stripping of 3D ocean-bottom-cable (OBC) PS-wave data over Valhall field, Olofsson et al. (2002) describe a dramatic "ring of anisotropy" in the overburden where the PS_1-wave is polarized transversely around the production platform. The correlation of this anisotropy pattern with sea-floor subsidence caused by the reservoir collapse after years of production suggests that shear waves are highly sensitive to local, deformation-induced stresses. Sensitivity of the polarization direction of the PS_1-wave to local stresses over anticlines has also been observed at Emilio field in the Adriatic Sea (Gaiser et al., 2002), and at Pinedale field in Wyoming, USA (Gaiser and Van Dok, 2005). As illustrated by Figure 8, the PS_1-wave at Emilio field is polarized parallel to the crest of a doubly plunging anticline (thick black arrows), where anisotropy is generally higher.

Finally, it is important to note that the moveout asymmetry of PS-waves (i.e., their traveltime generally does not stay the same when the source and receiver are interchanged) helps constrain the parameters of tilted TI media (Dewangan and Tsvankin, 2006b) and characterize dipping (non-vertical) fracture sets (Angerer et al., 2002).

Joint processing of PP and PS data

Conventional isotropic processing of high-quality multicomponent offshore OBC surveys routinely produces depth misties between PP and PS sections, in large part due to the strong influence of anisotropy on PS-wave moveout. The high sensitivity of mode conversions to anisotropy represents an asset for joint anisotropic inversion of PP and PS data (e.g., Grechka et al., 2002a; Foss et al., 2005). For example, the parameters V_{P0}, ϵ, and δ influence the kinematics of both P- and SV-waves in TI media, which underscores the importance of multicomponent data in anisotropic velocity analysis.

Widespread use of converted waves, however, is hindered not just by the higher acquisition cost of multicomponent surveys, but also

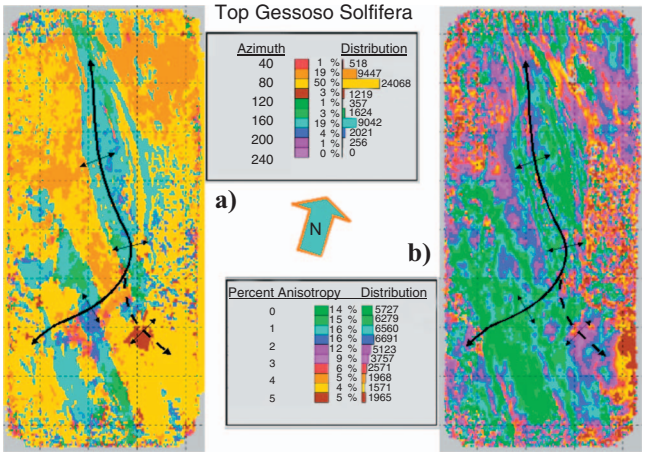

Figure 8. (a) Polarization azimuth of the PS_1-wave and (b) the shear-wave splitting coefficient (in percent) above the Gessoso Solfifera formation at Emilio field (after Gaiser et al., 2002). The north direction is rotated about 15° clockwise.

by difficulties in PS-wave processing. Such properties of mode conversions as moveout asymmetry, reflection point dispersal, and polarity reversals present significant challenges for velocity-analysis and imaging algorithms. These problems motivated the development of the so-called "PP + PS = SS" method designed to construct primary SS (in general, both S_1 and S_2) reflections with the correct kinematics from PP and PS data (Grechka and Tsvankin, 2002). The key idea of the method, which operates with PP and PS reflections acquired in split-spread geometry, is to match the time slopes (horizontal slownesses) of PP- and PS-waves on common-receiver gathers. This procedure helps identify PP and PS events reflected at the same (albeit unknown) subsurface points, and the SS-wave traveltime can be obtained as a simple linear combination of the PP and PS times. To avoid time picking, Grechka and Dewangan (2003) devised the full-waveform (interferometric) version of the PP + PS = SS method based on a specially designed convolution of PP and PS traces.

Although the PP + PS = SS method should be preceded by PP-PS event registration, it does not require information about the velocity field and is valid for arbitrarily anisotropic, heterogeneous media. The moveouts of the recorded PP-waves and computed SS-waves can be combined in anisotropic velocity analysis using, for example, 3D stacking-velocity tomography (Grechka et al., 2002a). The case study from the North Sea in Figure 9 demonstrates that this methodology greatly improves the quality of PS-wave stacked sections (Grechka et al., 2002b). Application of the PP + PS = SS method followed by VTI processing provided a much better image of the reservoir top (top Balder, the deepest arrow on the left) and a crisp picture of faulting in the shallow layers. Accounting for anisotropy also boosted higher frequencies in the stack and, therefore, increased temporal resolution.

FRACTURE CHARACTERIZATION

By some estimates, fractured reservoirs contain about one-third of the world's hydrocarbon reserves. Since aligned fractures create velocity and attenuation anisotropy on the scale of seismic wavelength, seismic fracture characterization is largely based on the anisotropic processing/inversion methods discussed above.

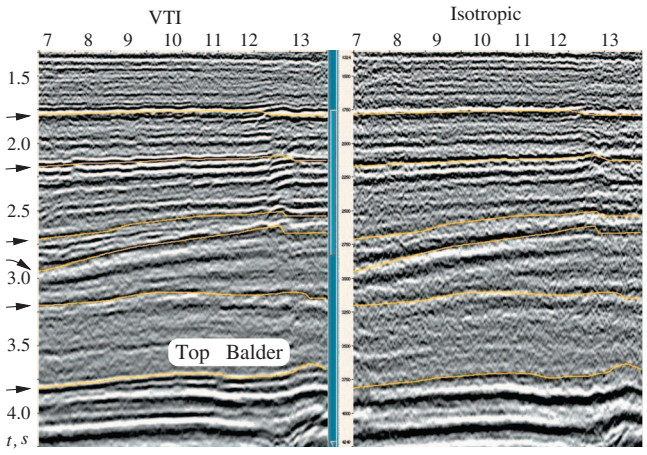

Figure 9. Common-conversion-point stacks of PSV-waves for a 2D line above the Siri reservoir in the North Sea (after Grechka et al., 2002b). Acquired PP- and PSV-waves were processed using the PP + PS = SS method to compute the traveltimes of the corresponding SS (SVSV) reflections. The section on the left was computed with a VTI velocity model obtained from stacking-velocity tomography of the recorded PP-waves and constructed SS-waves. The section on the right was produced without taking anisotropy into account.

In the past few years, significant progress has been achieved both in effective media theories and seismic characterization of multiple fracture sets. The theoretical advances are mainly attributed to increased computing power, which made it possible to construct so-called digital rocks and examine how such realistic features as crack intersections, shape irregularities, microcorrugation, and partial contacts of the fracture faces influence the effective elastic properties. It has been shown that multiple sets of irregular, possibly intersecting fractures that have random shape irregularities are well approximated by isolated, penny-shaped cracks (Grechka and Kachanov, 2006, and references therein).

Another important result, known from theoretical studies of Kachanov (1980, 1993) and confirmed numerically by Grechka et al. (2006), is that multiple, arbitrarily oriented sets of fractures embedded in an otherwise isotropic host rock yield an effective medium of approximately orthorhombic symmetry. This statement is valid for both dry and liquid-filled fractures. The former are close to so-called scalar cracks (in terminology of Schoenberg and Sayers, 1995), which always yield effective orthotropy (i.e., orthorhombic symmetry) in the non-interaction approximation. The latter contribute mainly to shear-wave anisotropy (i.e., to parameters analogous to the splitting coefficient $\gamma^{(S)}$) and also do not produce any substantial deviations from orthorhombic symmetry.

The closeness of the effective elasticity of cracked solids to orthotropy implies that multiple systems of fractures appear to long (compared to the fracture sizes) seismic waves as three orthogonal or principal sets. For instance, N sets of dry fractures that have the individual crack densities $e^{(k)}$ and the normals $n^{(k)}(k = 1,\ldots,N)$ to the fracture faces are equivalent to three "principal" sets, whose densities and orientations are found as the eigenvalues and eigenvectors of the crack-density tensor (Kachanov, 1980, 1993):

$$\alpha_{ij} = \sum_{k=1}^{N} e^{(k)} n_i^{(k)} n_j^{(k)}, \quad (i, j = 1, 2, 3). \tag{7}$$

Vasconcelos and Grechka (2007) employ this theory to characterize multiple vertical fracture sets from wide-azimuth, multicomponent seismic reflection data recorded at Rulison field. The fracture orientations obtained from seismic data are consistent with the FMI (Formation MicroImager) log acquired in the study area. In addition, Vasconcelos and Grechka (2007) construct an orthorhombic velocity model of the Rulison reservoir by jointly inverting P- and S-wave NMO ellipses. This inversion is possible primarily because crack-induced orthotropy is governed by fewer independent parameters than general orthorhombic media, making estimation of these parameters better posed and easier to implement. Still, comparison of the spatially varying crack densities with the estimated ultimate recovery (EUR) of the available wells shows little correlation. This problem, typical for a number of other tight-gas fields in North America, should motivate further development of robust seismic technologies capable of detecting accumulations of hydrocarbons in fractured formations.

THE ROAD AHEAD

Progress in geophysics is usually driven by data; whenever we acquire a new type of data, we can expect to discover unexpected fea-

tures that cannot be handled by existing methodologies. In hindsight, these surprises should have been foreseen (and maybe were foreseen by a few savants), but they always do surprise most of us.

Today, the industry routinely acquires high-quality wide-azimuth 3D marine data with the goal of better illuminating subsalt targets. When processing such data, we are discovering that azimuthally variable seismic velocity is often required to flatten the wide-azimuth image gathers. This will surely lead us to further develop methods dealing with azimuthal anisotropy, which have been applied primarily to land data sets. Also, it is already clear that horizontal transverse isotropy (HTI) is not an appropriate model for most formations with vertical cracks, and TTI is probably an oversimplified symmetry for dipping beds. Future developments will include extension of velocity-analysis and migration algorithms to more realistic orthorhombic models. Although a solid foundation for parameter estimation and imaging in orthorhombic media has already been built, finding robust and cost-effective processing solutions is a serious challenge, especially for tilted orthotropy. Also, it would not be practical to operate with a parameter set that is not constrained by available seismic data. Another direction of future research with a high potential payoff in velocity analysis is anisotropic full-waveform inversion of reflection data, which should become feasible with continuing increase in computing power.

An interesting feature of anisotropy is that, although usually it is weak (i.e., the dimensionless anisotropy parameters typically are much smaller than unity), in many contexts it has a strong influence on seismic data. In particular, the contribution of anisotropy to reflection coefficients is comparable to the isotropic "fluid" and "lithology" factors, which is particularly noticeable in the azimuthally varying P-wave AVO response. Anisotropy in the overburden also causes pronounced distortions in the geometric-spreading factor for reflected waves. Hence, it is easy to predict that more emphasis will be placed on understanding and utilizing amplitude signatures in anisotropic media, likely including attenuation measurements. Experimental data indicate that attenuation anisotropy, especially that produced by fluid-saturated fractures, may be orders of magnitude higher than velocity anisotropy. Therefore, azimuthally varying (and, possibly, frequency-dependent) attenuation coefficients may provide sensitive reservoir-characterization attributes.

Anisotropic phenomena are especially noticeable in shear and mode-converted wavefields; it is usually impossible to deal with shear data without considering anisotropy. In so doing, completely new concepts (unknown in isotropy) arise, such as shear-wave splitting. For example, acquisition of high-quality PS-wave data in recent years revealed strong conversion of energy (P-to-S) at near-normal incidence, which is prohibited by the standard model of plane-wave reflection from a planar boundary between isotropic or VTI halfspaces. Some of candidate explanations of these anomalous PS arrivals involve anisotropy (e.g., tilted TI on either side of the reflector). Whatever the eventual solution to this problem, it will likely entail a revision of conventional AVO models and algorithms for both PP- and PS-waves. Also, wide-azimuth, multicomponent data will play a major role in robust parameter estimation for realistic orthorhombic and, in some cases, lower-symmetry media. Note that the split shear-wave primary reflections (S_1 and S_2) with the correct kinematics can be generated from wide-azimuth PP and PS data using the 3D version of the PP + PS = SS method.

Whereas anisotropic P-wave imaging essentially amounts to looking "past" anisotropy at exploration targets, progress in processing/inversion techniques is putting more emphasis on employing anisotropy parameters as attributes in reservoir characterization and lithology discrimination. One of interesting emerging applications of anisotropic attributes is in time-lapse seismic for compacting reservoirs because the shear-wave splitting coefficient, traveltime shifts and other compaction-related signatures are strongly influenced by stress-induced anisotropy. Physical characterization of the subsurface in terms of lithology, fluids, fractures, pore pressure, and permeability will require improved rock-physics and geomechanics methods operating with anisotropic models.

ACKNOWLEDGMENTS

We are grateful to our numerous colleagues for their contributions discussed in the paper and for fruitful discussions that improved our understanding of the subject. We appreciate the reviews by K. Helbig, A. Rüger, and A. Stovas, who made a number of helpful suggestions. I.T. acknowledges the support of the Center for Wave Phenomena at Colorado School of Mines.

REFERENCES

Alford, R. M., 1986, Shear data in the presence of azimuthal anisotropy: 56th Annual International Meeting, SEG, Expanded Abstracts, 476–479.
Alkhalifah, T., 1997, Seismic data processing in vertically inhomogeneous TI media: Geophysics, **62**, 662–675.
Alkhalifah, T., and I. Tsvankin, 1995, Velocity analysis for transversely isotropic media: Geophysics, **60**, 1550–1566.
Alkhalifah, T., I. Tsvankin, K. Larner, and J. Toldi, 1996, Velocity analysis and imaging in transversely isotropic media: Methodology and a case study: The Leading Edge, **15**, 371–378.
Anderson, J. E., T. Alkhalifah, and I. Tsvankin, 1996, Fowler DMO and time migration for transversely isotropic media: Geophysics, **61**, 835–844.
Angerer, E., S. Crampin, X.-Y. Li, and T. L. Davis, 2000, Time-lapse seismic changes in a CO_2 injection process in a fractured reservoir: 70th Annual International Meeting, SEG, Expanded Abstracts, 1532–1535.
Angerer, E., S. A. Horne, J. E. Gaiser, R. Walters, S. Bagala, and L. Vetri, 2002, Characterization of dipping fractures using PS mode-converted data: 72nd Annual International Meeting, SEG, Expanded Abstracts, 1010–1013.
Auld, B. A., 1973, Acoustic fields and waves in solids: J. Wiley and Sons.
Backus, G. E., 1962, Long-wave elastic anisotropy produced by horizontal layering: Journal of Geophysical Research, **67**, 4427–4440.
Bakulin, A., V. Grechka, and I. Tsvankin, 2000, Estimation of fracture parameters from reflection seismic data — Parts I, II, and III: Geophysics, **65**, 1788–1830.
Bakulin, A., M. Woodward, D. Nichols, K. Osypov, and O. Zdraveva, 2009, Building TTI depth models using anisotropic tomography with well information: 79th Annual International Meeting, SEG, Expanded Abstracts, Paper TOM 2.6.
Bale, R., B. Gratakos, B. Mattocks, S. Roche, K. Poplavskii, and X. Li, 2009, Shear wave splitting applications for fracture analysis and improved imaging: Some onshore examples: First Break, **27**, 73–83.
Ball, G., 1995, Estimation of anisotropy and anisotropic 3-D prestack migration, offshore Zaire: Geophysics, **60**, 1495–1513.
Banik, N. C., 1987, An effective parameter in transversely isotropic media: Geophysics, **52**, 1654–1664.
Bear, L. K., T. A. Dickens, J. R. Krebs, J. Liu, and P. Traynin, 2005, Integrated velocity model estimation for improved positioning with anisotropic PSDM: The Leading Edge, **24**, 622–626.
Behera, L., and I. Tsvankin, 2009, Migration velocity analysis for tilted transversely isotropic media: Geophysical Prospecting, **57**, 13–26.
Behura, J., and I. Tsvankin, 2009, Estimation of interval anisotropic attenuation from reflection data: Geophysics, **74**, no. 6, A69–A74.
Booth, D. C., and S. Crampin, 1983, The anisotropic reflectivity method: Theory: Geohysical Journal of the Royal Astronomical Society, **72**, 755–766.
Buchwald, V., 1959, Elastic waves in anisotropic media: Proceedings of the Royal Society of London, A, **235**, 563–580.
Byun, B. S., D. Corrigan, and J. E. Gaiser, 1989, Anisotropic velocity analysis for lithology discrimination: Geophysics, **54**, 1564–1574.
Carcione, J., D. Kosloff, and R. Kosloff, 1988, Wave-propagation simulation in anelastic anisotropic (transversely isotropic) solid: Journal of Mechanics and Applied Mathematics, **41**, 319–345.
Carcione, J., G. C. Herman, and A. P. E. ten Kroode, 2002, Seismic modeling:

Geophysics, **67**, 1304–1325.
Červený, V., 1972, Seismic rays and ray intensities in inhomogeneous anisotropic media: Geophysical Journal of the Royal Astronomical Society, **29**, 1–13.
———, 2001, Seismic ray theory: Cambridge University Press.
Chapman, C. H., 2004, Fundamentals of seismic wave propagation: Cambridge University Press.
Chapman, M., 2003, Frequency-dependent anisotropy due to mesoscale fractures in the presence of equant porosity: Geophysical Prospecting, **51**, 369–379.
Chichinina, T., I. Obolentseva, L. Gik, B. Bobrov, and G. Ronquillo-Jarillo, 2009, Attenuation anisotropy in the linear-slip model: Interpretation of physical modeling data: Geophysics, **74**, no. 5, WB165–WB176.
Clark, R. A., P. M. Benson, A. J. Carter, and C. A. Guerrero Moreno, 2009, Anisotropic P-wave attenuation measured from a multi-azimuth surface seismic reflection survey: Geophysical Prospecting, **57**, 835–845.
Corrigan, D., R. Withers, J. Darnall, and T. Skopinski, 1996, Fracture mapping from azimuthal velocity analysis using 3-D surface seismic data: 66th Annual International Meeting, SEG, Expanded Abstracts, 1834–1837.
Crampin, S., 1981, A review of wave motion in anisotropic and cracked elastic media: Wave Motion, **3**, 343–391.
Crampin, S., 1985, Evaluation of anisotropy by shear-wave splitting: Geophysics, **50**, 142–152.
Crampin, S., 2003, The New Geophysics: Shear-wave splitting provides a window into the crack-critical rock mass: The Leading Edge, **22**, 536–549.
Daley, P., and F. Hron, 1977, Reflection and transmission coefficients for transversely isotropic media: Bulletin of the Seismological Society of America, **67**, 661–675.
Dellinger, J., S. Brandsberg-Dahl, R. Clarke, and L. Thomsen, 2002, Alford rotation after tensor migration: 72nd Annual International Meeting, SEG, Expanded Abstracts, 982–985.
de Nicolao, A., G. Drufuca, and F. Rocca, 1993, Eigenvectors and eigenvalues of linearized elastic inversion: Geophysics, **58**, 670–679.
de Parscau, J., 1991, P- and SV-wave transversely isotropic phase velocity analysis from VSP data: Geophysical Journal International, **107**, 629–638.
DeVault, B., T. L. Davis, I. Tsvankin, R. Verm, and F. Hilterman, 2002, Multicomponent AVO analysis, Vacuum field, New Mexico: Geophysics, **67**, 701–710.
Dewangan, P., and V. Grechka, 2003, Inversion of multicomponent, multiazimuth, walkaway VSP data for the stiffness tensor: Geophysics, **68**, 1022–1031.
Dewangan, P., and I. Tsvankin, 2006a, Velocity-independent layer stripping of PP and PS reflection traveltimes: Geophysics, **71**, no. 4, U59–U65.
———, 2006b, Modeling and inversion of PS-wave moveout asymmetry for tilted TI media: Part 1 — Horizontal TTI layer: Geophysics, **71**, no. 4, D107–D122.
Douma, H., and M. van der Baan, 2008, Rational interpolation of qP-traveltimes for semblance-based anisotropy estimation in layered VTI media: Geophysics, **73**, no. 4, D53–D62.
Dunne, J., and G. Beresford, 1998, Improving seismic data quality in the Gippsland Basin (Australia): Geophysics, **63**, 1496–1506.
Fomel, S., 2004, On anelliptic approximations for qP velocities in VTI media: Geophysical Prospecting, **52**, 247–259.
Foss, S.-K., B. Ursin, and M. V. de Hoop, 2005, Depth-consistent reflection tomography using PP and PS seismic data: Geophysics, **70**, no. 5, U51–U65.
Fowler, P. J., A. Jackson, J. Gaffney, and D. Boreham, 2008, Direct nonlinear traveltime inversion in layered VTI media: 78th Annual International Meeting, SEG, Expanded Abstracts, 3028–3032.
Fryer, G. J., 1980, A slowness approach to the reflectivity method for seismogram synthesis: Geophysical Journal of the Royal Astronomical Society, **63**, 747–758.
Fryer, G. J., and L. N. Frazer, 1984, Seismic waves in stratified anisotropic media: Geophysical Journal of the Royal Astronomical Society, **78**, 691–710.
Fuchs, K., and G. Müller, 1971, Computation of synthetic seismograms with the reflectivity method and comparison with observations: Geophysical Journal of the Royal Astronomical Society, **23**, 417–433.
Gaiser, J. E., 1990, Transversely isotropic phase velocity analysis from slowness estimates: Journal of Geophysical Research, **95**, 11241–11254.
———, 1997, 3-D converted shear wave rotation with layer stripping: U.S. Patent 5,610,875.
———, 1999, Enhanced PS-wave images and attributes using prestack azimuth processing: 69th Annual International Meeting, SEG, Expanded Abstracts, 699–702.
———, 2000, Advantages of 3-D PS-wave data to unravel S-wave birefringence for fracture detection: 70th Annual International Meeting, SEG, Expanded Abstracts, 1201–1204.
Gaiser, J. E., and R. Van Dok, 2005, Borehole calibration of PS-waves for fracture characterization: Pinedale field, Wyoming: 75th Annual International meeting, SEG, Expanded Abstracts, 873–876.
Gaiser, J. E., E. Loinger, H. Lynn, and L. Vetri, 2002, Birefringence analysis at Emilio field for fracture characterization: First Break, **20**, 505–514.
Gajewski, D., and I. Pšenčík, 1987, Computation of high-frequency seismic wavefields in 3-D laterally inhomogeneous anisotropic media: Geophysical Journal of the Royal Astronomical Society, **91**, 383–411.
Garotta, R., and P. Y. Granger, 1988, Acquisition and processing of 3C × 3D data using converted waves: 58th Annual International Meeting, SEG, Expanded Abstracts, 995–998.
Gilbert, F., and G. E. Backus, 1966, Propagator matrices in elastic wave and vibration theory: Geophysics, **31**, 326–332.
Gray, F. D., and D. Todorovic-Marinic, 2004, Fracture detection using 3D azimuthal AVO: CSEG Recorder, **29**, 5–8.
Gray, F. D., G. Roberts, and K. J. Head, 2002, Recent advances in determination of fracture strike and crack density from P-wave seismic data: The Leading Edge, **21**, 280–285.
Grechka, V., 2009, Applications of seismic anisotropy in the oil and gas industry: European Association of Geoscientists and Engineers.
Grechka, V., and P. Dewangan, 2003, Generation and processing of pseudo shear-wave data: Theory and case study: Geophysics, **68**, 1807–1816.
Grechka, V., and M. Kachanov, 2006, Effective elasticity of fractured rocks: A snapshot of the work in progress: Geophysics, **71**, no. 6, W45–W58.
Grechka, V., and A. Mateeva, 2007, Inversion of P-wave VSP data for local anisotropy: Theory and a case study: Geophysics, **72**, no. 4, D69–D79.
Grechka, V., and I. Tsvankin, 1998, 3-D description of normal moveout in anisotropic inhomogeneous media: Geophysics, **63**, 1079–1092.
———, 1999, 3-D moveout inversion in azimuthally anisotropic media with lateral velocity variation: Theory and a case study: Geophysics, **64**, 1202–1218.
———, 2002, PP + PS = SS: Geophysics, **67**, 1961–1971.
Grechka, V., P. Contreras, and I. Tsvankin, 2000, Inversion of normal moveout for monoclinic media: Geophysical Prospecting, **48**, 577–602.
Grechka, V., A. Pech, and I. Tsvankin, 2002a, Multicomponent stacking-velocity tomography for transversely isotropic media: Geophysics, **67**, 1564–1574.
———, 2005, Parameter estimation in orthorhombic media using multicomponent wide-azimuth reflection data: Geophysics, **70**, no. 2, D1–D8.
Grechka, V., I. Tsvankin, and J. K. Cohen, 1999, Generalized Dix equation and analytic treatment of normal-moveout velocity for anisotropic media: Geophysical Prospecting, **47**, 117–148.
Grechka, V., I. Vasconcelos, and M. Kachanov, 2006, The influence of crack shape on the effective elasticity of fractured rocks: Geophysics, **71**, no. 5, D153–D160.
Grechka, V., I. Tsvankin, A. Bakulin, C. Signer, and J. O. Hansen, 2002b, Anisotropic inversion and imaging of PP and PS reflection data in the North Sea: The Leading Edge, **21**, 90–97.
Grechka, V., A. Mateeva, G. Franco, C. Gentry, P. Jorgensen, and J. Lopez, 2007, Estimation of seismic anisotropy from P-wave VSP data: The Leading Edge, **26**, 756–759.
Haacke, R. R., G. K. Westbrook, and S. Peacock, 2009, Layer stripping of shear-wave splitting in marine PS-waves: Geophysical Journal International, **176**, 782–804.
Hake, H., 1986, Slant stacking and its significance for anisotropy: Geophysical Prospecting, **34**, 595–608.
Hall, S., and J. M. Kendall, 2003, Fracture characterization at Valhall: Application of P-wave amplitude variation with offset and azimuth (AVOA) analysis to a 3-D ocean-bottom data set: Geophysics, **68**, 1150–1160.
Haskell, N. A., 1953, The dispersion of surface waves on multilayer media: Bulletin of the Seismological Society of America, **43**, 17–34.
Helbig, K., 1994, Foundations of elastic anisotropy for exploration seismics: Pergamon Press.
Helbig, K., and L. Thomsen, 2005, 75–plus years of anisotropy in exploration and reservoir seismics: A historical review of concepts and methods: Geophysics, **70**, no. 6, 9ND–23ND.
Hess, H. H., 1964, Seismic anisotropy of the uppermost mantle under oceans: Nature, **203**, 629–631.
Horne, S., and S. Leaney, 2000, Short note: Polarization and slowness component inversion for TI anisotropy: Geophysical Prospecting, **48**, 779–788.
Hsu, K., M. Schoenberg, and J. Walsh, 1991, Anisotropy from polarization and moveout: 61st Annual International Meeting, SEG, Expanded Abstracts, 1526–1529.
Huang, T., Y. Zhang, H. Zhang, and J. Young, 2009, Subsalt imaging using TTI reverse time migration: The Leading Edge, **28**, 448–452.
Jenner, E., 2001, Azimuthal anisotropy of 3-D compressional wave seismic data, Weyburn field, Saskatchewan, Canada: Ph.D. thesis, Colorado School of Mines.
———, 2009, Data example and modelling study of P-wave azimuthal anisotropy potentially caused by isotropic velocity heterogeneity: First Break, **27**, 45–50.
Ji, Y., and S. C. Singh, 2005, Anisotropy from full waveform inversion of multicomponent seismic data using a hydrid optimization method: Geophysical Prospecting, **53**, 435–445.

Jílek, P., 2002a, Converted PS-wave reflection coefficients in weakly anisotropic media: Pure and Applied Geophysics, **159**, 1527–1562.
———, 2002b, Modeling and inversion of converted-wave reflection coefficients in anisotropic media: A tool for quantitative AVO analysis: Ph.D. thesis, Colorado School of Mines.
Jílek, P., B. Hornby, and A. Ray, 2003, Inversion of 3D VSP P-wave data for local anisotropy: A case study: 73rd Annual Meeting, SEG, Expanded Abstracts, 1322–1325.
Kachanov, M., 1980, Continuum model of medium with cracks: Journal of the Engineering Mechanics Division, ASCE, **106** (EM5), 1039–1051.
———, 1993, Elastic solids with many cracks and related problems, *in* J. W. Hutchinson and T. Wu, eds., Advances in Applied Mechanics, 30, 259–445.
Keith, C. M., and S. Crampin, 1977, Seismic body waves in anisotropic media: Synthetic seismograms: Geophysical Journal of the Royal Astronomical Society, **49**, 225–243.
Kennett, B. L. N., 1972, Reflections, rays, and reverberations: Bulletin of the Seismological Society of America, **64**, 1685–1696.
———, 1983, Seismic wave propagation in stratified media: Cambridge University Press.
Komatitsch, D., and J. Tromp, 1999, Introduction to the spectral-element method for 3-D seismic wave propagation: Geophysical Journal International, **139**, 806–822.
Komatitsch, D., C. Barnes, and J. Tromp, 2000, Simulation of anisotropic wave propagation based upon a spectral element method: Geophysics, **65**, 1251–1260.
Kormendi, F., and M. Dietrich, 1991, Nonlinear waveform inversion of plane-wave seismograms in stratified elastic media: Geophysics, **56**, 664–674.
Kosloff, D., and E. Baysal, 1982, Forward modeling by the Fourier method: Geophysics, **47**, 1402–1412.
Li, X.-Y., and C. MacBeth, 1999, Fracture detection with marine P-S mode conversion: Proceedings of the Offshore Technology Conference, Houston, TX, Paper no. 10941-MS.
Lighthill, M. J., 1960, Study of magneto-hydrodynamic waves and other anisotropic wave motions: Philosophical Transactions of the Royal Society of London, A, **252**, 397–430.
Lynn, H. B., and L. Thomsen, 1986, Shear wave exploration along the principal axis: 56th Annual International Meeting, SEG, Expanded Abstracts, 474–476.
Lynn, H. B., D. Campagna, K. M. Simon, and W. E. Beckham, 1999, Relationship of P-wave seismic attributes, azimuthal anisotropy, and commercial gas pay in 3-D P-wave multiazimuth data, Rulison Field, Piceance Basin, Colorado: Geophysics, **64**, 1293–1311.
Mah, M., and D. R. Schmitt, 2003, Determination of complete elastic stiffnesses from ultrasonic phase velocity measurements: Journal of Geophysical Research, **108** (B1), 2016.
Mallick, S., and L. N. Frazer, 1991, Reflection/transmission coefficients and azimuthal anisotropy in marine seismic studies: Geophysical Journal International, **105**, 241–252.
Martin, M. A., and T. L. Davis, 1987, Shear-wave birefringence: A new tool for evaluating fractured reservoirs: The Leading Edge, **6**, 22–28.
Martinez, R. D., 1993, Wave propagation effects on amplitude variation with offset measurements: A modeling study: Geophysics, **58**, 534–543.
Martinez, R. D., and G. A. McMechan, 1991, τ-p seismic for viscoelastic media — Part 2: Linearized inversion: Geophysical Prospecting, **39**, 157–181.
Maultzsch, S., M. Chapman, E. Liu, and X.-Y. Li, 2009, Anisotropic attenuation in VSP data: Journal of Seismic Exploration, **16**, 145–158.
Maultzsch, S., S. Horne, S. Archer, and H. Burkhardt, 2003, Effects of an anisotropic overburden on azimuthal amplitude analysis in horizontal transversely isotropic media: Geophysical Prospecting, **51**, 61–74.
Mensch, T., and P. Rasolofosaon, 1997, Elastic-wave velocities in anisotropic media of arbitrary symmetry — generalization of Thomsen's parameters ϵ, δ, and γ: Geophysical Journal International, **128**, 43–64.
Miller, D. E., and C. Spencer, 1994, An exact inversion for anisotropic moduli from phase slowness data: Journal of Geophysical Research, **99**, 21651–21657.
Mueller, M. C., 1991, Prediction of lateral variability in fracture intensity using multicomponent shear-wave surface seismic as a precursor to horizontal drilling in the Austin Chalk: Geophysical Journal International, **107**, 409–416.
Müller, G., 1971, Direct inversion of seismic observations: Journal of Geophysics, **37**, 225–235.
Musgrave, M. J. P., 1970, Crystal acoustics: Introduction to the study of elastic waves and vibrations in crystals: Holden-Day.
Neal, S., N. R. Hill, and Y. Wang, 2009, Anisotropic velocity modeling and prestack Gaussian-beam depth migration with applications in the deepwater Gulf of Mexico: The Leading Edge, **28**, 1110–1119.
Olofsson, B., J. Kommedal, O. Barkved, R. Alexandre, J. E. Brunelliere, and E. Muyzert, 2002, Continuous progress in processing multicomponent data — A case study: 64th Annual EAGE meeting, Extended Abstracts, Paper F-22.
Reine, C. A., R. A. Clark, and M. van der Baan, 2009, Interval-Q measurements from surface seismic data using a robust prestack inversion algorithm: 71st Annual Meeting, EAGE, Extended Abstracts, Paper S041.
Ren, J., C. Gerrard, J. McClean, and M. Orlovich, 2005, Prestack wave-equation depth migration in VTI media: The Leading Edge, **24**, 618–620.
Rüger, A., 1997, P-wave reflection coefficients for transversely isotropic models with vertical and horizontal axis of symmetry: Geophysics, **62**, 713–722.
———, 1998, Variation of P-wave reflectivity with offset and azimuth in anisotropic media: Geophysics, **63**, 935–947.
———, 2002, Reflection coefficients and azimuthal AVO analysis in anisotropic media: Society of Exploration Geophysicists.
Sarkar, D., and I. Tsvankin, 2004, Migration velocity analysis in factorized VTI media: Geophysics, **69**, 708–718.
———, 2006, Anisotropic migration velocity analysis: Application to a data set from West Africa: Geophysical Prospecting, **54**, 575–587.
Schoenberg, M., and C. Sayers, 1995, Seismic anisotropy of fractured rock: Geophysics, **60**, 204–211.
Sena, A. G., 1991, Seismic traveltime equations for azimuthally anisotropic and isotropic media: Estimation of interval elastic properties: Geophysics, **56**, 2090–2101.
Sena, A. G., and M. N. Toksöz, 1993, Kirchhoff migration and velocity analysis for converted and nonconverted waves in anisotropic media: Geophysics, **58**, 265–276.
Simmons, J. L., 2009, Converted-wave splitting estimation and compensation: Geophysics, **74**, no. 1, D37–D48.
Stoffa, P. L., J. B. Diebold, and P. Buhl, 1981, Inversion of seismic data in the τ-p domain: Geophysical Research Letters, **8**, 869–872.
———, 1982, Velocity analysis of wide aperture seismic data: Geophysical Prospecting, **30**, 25–57.
Stovas, A., and B. Ursin, 2009, Improved geometric-spreading approximation in layered transversely isotropic media: Geophysics, **74**, no. 5, D85–D95.
Terrell, M. J., T. L. Davis, L. T. Brown, and R. F. Fuck, 2002, Seismic monitoring of a CO2 flood at Weyburn field, Saskatchewan: Demonstrating the robustness of time-lapse seismology: 72nd Annual International Meeting, SEG, Expanded Abstracts, 1673–1676.
Thomsen, L., 1986, Weak elastic anisotropy: Geophysics, **51**, 1954–1966.
———, 1993, Weak anisotropic reflections, *in* Castagna J. and M. Backus, eds., Offset dependent reflectivity, 103–114, SEG.
———, 1999, Converted-wave reflection seismology over inhomogeneous, anisotropic media: Geophysics, **64**, 678–690.
———, 2002, Understanding seismic anisotropy in exploration and exploitation: SEG/EAGE Distinguished Instructor Series.
Thomsen, L., I. Tsvankin, and M. C. Mueller, 1999, Coarse-layer stripping of vertically variable azimuthal anisotropy from shear-wave data: Geophysics, **64**, 1126–1138.
Tod, S., B. Taylor, R. Johnston, and T. Allen, 2007, Fracture prediction from wide-azimuth land seismic data in SE Algeria: The Leading Edge, **26**, 1154–1160.
Toldi, J., T. Alkhalifah, P. Berthet, J. Arnaud, P. Williamson, and B. Conche, 1999, Case study of estimation of anisotropy: The Leading Edge, **18**, 588–594.
Treitel, S., P. R. Gutowski, and D. E. Wagner, 1982, Plane-wave decomposition of seismograms: Geophysics, **47**, 1375–1401.
Tsvankin, I., 1995a, Seismic wavefields in layered isotropic media: Samizdat Press, Colorado School of Mines.
———, 1995b, Body-wave radiation patterns and AVO in transversely isotropic media: Geophysics, **60**, 1409–1425.
———, 1997, Anisotropic parameters and P-wave velocity for orthorhombic media: Geophysics, **62**, 1292–1309.
———, 2005, Seismic signatures and analysis of reflection data in anisotropic media, 2nd ed.: Elsevier Science Publ. Co., Inc.
Tsvankin, I., and E. M. Chesnokov, 1990, Synthesis of body-wave seismograms from point sources in anisotropic media: Journal of Geophysical Research, **95** (B7), 11317–11331.
Tsvankin, I., and L. Thomsen, 1994, Nonhyperbolic reflection moveout in anisotropic media: Geophysics, **59**, 1290–1304.
Ursin, B., and K. Hokstad, 2003, Geometrical spreading in a layered transversely isotropic medium with vertical symmetry axis: Geophysics, **68**, 2082–2091.
Ursin, B., and A. Stovas, 2006, Traveltime approximations for a layered transversely isotropic medium: Geophysics, **71**, no. 2, D23–D33.
van der Baan, M., 2004, Processing of anisotropic data in the τ-p domain: I — Geometric spreading and moveout corrections: Geophysics, **69**, 719–730.
———, 2005, Processing of anisotropic data in the τ-p domain: II — Common-conversion-point sorting: Geophysics, **70**, no. 4, D29–D36.
———, 2006, PP/PS wavefield separation by independent component analysis: Geophysical Journal International, **166**, 339–348.
van der Baan, M., and J.-M. Kendall, 2002, Estimating anisotropy parame-

ters and traveltimes in the τ-p domain: Geophysics, **67**, 1076–1086.
——–, 2003, Traveltime and conversion-point computations and parameter estimation in layered, anisotropic media by τ-p transform: Geophysics, **68**, 210–224.
van der Baan, M., and D. Smit, 2006, Amplitude analysis of isotropic P-wave reflections: Geophysics, **71**, no. 6, C93–C103.
Vanelle, C., and D. Gajewski, 2003, Determination of geometrical spreading from traveltimes: Journal of Applied Geophysics, **54**, 391–400.
Vasconcelos, I., and V. Grechka, 2007, Seismic characterization of multiple fracture sets at Rulison Field, Colorado: Geophysics, **72**, no. 2, B19–B30.
Vasconcelos, I., and I. Tsvankin, 2006, Nonhyperbolic moveout inversion of wide-azimuth P-wave data for orthorhombic media: Geophysical Prospecting, **54**, 535–552.
Vavryčuk, V., and I. Pšenčík, 1998, PP-wave reflection coefficients in weakly anisotropic elastic media: Geophysics, **63**, 2129–2141.
Vestrum, R. W., D. C. Lawton, and R. Schmid, 1999, Imaging structures below dipping TI media: Geophysics, **64**, 1239–1246.
Virieux, J., 1986, P-SV propagation in heterogeneous media — Velocity-stress finite-difference method: Geophysics, **51**, 889–901.
Vlaar, N. J., 1968, Ray theory for an anisotropic inhomogeneous elastic medium: Bulletin of the Seismological Society of America, **58**, 2053–2072.
Wang, D. Y., and D. W. McCowan, 1989, Spherical divergence correction for seismic reflection data using slant stacks: Geophysics, **54**, 563–569.
Wang, X., and I. Tsvankin, 2009, Estimation of interval anisotropy parameters using velocity-independent layer stripping: Geophysics, **74**, no. 5, WB117–WB127.
Wang, Z., 2002, Seismic anisotropy in sedimentary rocks, part 2: Laboratory data: Geophysics, **67**, 1423–1440.
White, J. E., L. Martineau-Nicoletis, and C. Monash, 1983, Measured anisotropy in Pierre shale: Geophysical Prospecting, **31**, 709–725.
Willis, H., G. Rethford, and E. Bielanski, 1986, Azimuthal anisotropy: The occurence and effect on shear wave data quality: 56th Annual International Meeting, SEG, Expanded Abstracts, 479–481.
Winterstein, D. F., and M. A. Meadows, 1991, Changes in shear-wave polarization azimuth with depth in Cymric and Railroad Gap oil fields: Geophysics, **56**, 1349–1364.
Woodward, M. J., D. Nichols, O. Zdraveva, P. Whitfield, and T. Johns, 2008, A decade of tomography: Geophysics, **73**, no. 5, VE5–VE11.
Xu, X., and I. Tsvankin, 2006, Anisotropic geometrical-spreading correction for wide-azimuth P-wave reflections: Geophysics, **71**, no. 5, D161–D170.
——–, 2007, A case study of azimuthal AVO analysis with anisotropic spreading correction: The Leading Edge, **26**, 1552–1561.
——–, 2008, Moveout-based geometrical-spreading correction for PS-waves in layered anisotropic media: Journal of Geophysics and Engineering, **5**, 195–202.
Zatsepin, S. V., and S. Crampin, 1997, Modelling the compliance of crustal rock: I — Response of shear-wave splitting to differential stress: Geophysical Journal International, **129**, 477–494.
Zhu, T., S. H. Gray, and D. Wang, 2007a, Prestack Gaussian-beam depth migration in anisotropic media: Geophysics, **72**, no. 3, S133–S138.
Zhu, Y., and I. Tsvankin, 2006, Plane-wave propagation in attenuative transversely isotropic media: Geophysics, **71**, no. 2, T17–T30.
——–, 2007, Plane-wave attenuation anisotropy in orthorhombic media: Geophysics, **72**, no. 1, D9–D19.
Zhu, Y., I. Tsvankin, P. Dewangan, and K. van Wijk, 2007b, Physical modeling and analysis of P-wave attenuation anisotropy in transversely isotropic media: Geophysics, **72**, no. 1, D1–D7.